

## Electrochemical Synthesis, Characterization and Corrosion Properties of POA – MoO<sub>4</sub><sup>2-</sup> Coating in 3.5% NaCl

Ye.G. Bakhytzhn, A.M. Argimbayeva\*, G.S. Rakhymbay,  
R.Dzh. Jumanova, Kh. Avchukir, B.D. Burkitbayeva

Al-Farabi Kazakh National University, 71 al-Farabi Ave., Almaty, Kazakhstan

### Article info

Received:  
10 February 2020

Received in revised form:  
15 April 2020

Accepted:  
17 June 2020

### Abstract

Polyaniline (POA) and polyaniline-molybdate ( POA – MoO<sub>4</sub><sup>2-</sup> ) coatings have been successfully synthesized on steel grade CT3 from aqueous solutions of oxalic acid by electrochemical method using cyclic voltammetry. The morphology and composition of these films were characterized by scanning electron microscopy (SEM) and energy-dispersive X-ray (EDAX) methods. It was proven that the introduction of MoO<sub>4</sub><sup>2-</sup> into the polyaniline matrix raised the corrosion resistance of the POA coating and also improved its adhesion properties. The protective properties of steel grade CT3 with POA and POA – MoO<sub>4</sub><sup>2-</sup> films were studied using potentiodynamic polarization in 3.5% NaCl solution. The results showed that MoO<sub>4</sub><sup>2-</sup> ions improve anti-corrosion properties of POA films.

### 1. Introduction

CT3 mild steel is the main structural material in many industrial installations, in particular, in the metal, oil and gas industries, as well as in wastewater treatment plants [1–3], due to a number of advantages including ease of manufacturing, availability, high strength and low cost [4, 5]. However, in corrosive environments involving acids or seawater, the service life of mild steel structures is greatly reduced by corrosive processes on the metal surface. To minimize the corrosion of steel in these environments, there is a need to develop new solutions.

Inhibitory protection is one of the available, simple and effective methods of protecting metals from corrosion. A large number of compounds and compositions having a good protective ability have now been proposed. However, not all proposed inhibitors are environmentally friendly and economically viable. The main disadvantage of most organic and inorganic corrosion inhibitors is their toxicity, which leads to adverse effects on the environment and human health. As a result of

searching for alternative corrosion inhibitors, conducting polymers were proposed [6]. The use of organic polymer coatings is found as a preference due to advantages like environmental friendliness, ease to synthetic methods and high conductivity [7, 8]. These films can be obtained also by the electrochemical method, which allows the control of properties resulting from coatings such as coating thickness, conductive properties, etc. [9–11].

Conductive polymers such as polypyrrole, polyaniline, polythiophene have attracted great interest due to their high protective effect and conductivity [4, 6]. With a number of advantages including – low cost, availability and environmental friendliness. Aniline monomer having a methoxy group in the ortho position is a derivative of the aniline group. Due to its high solubility in an aqueous medium, the electrochemical method of synthesis of POA from aqueous solution eliminates the use of toxic organic solvents and therefore no need for waste disposal. In addition, the conversion of monomer to polymer is not difficult [13, 14]. The authors of an investigation of the corrosion behavior of grade 304 steel during the electrochemical synthesis of POA coatings [12] found out that polyaniline decreases the corrosion rate of steel as much as 15 times in a solution containing chloride ions.

\*Corresponding author.

E-mail: [akmaral.argimbayeva@gmail.com](mailto:akmaral.argimbayeva@gmail.com)

Despite the high anti-corrosion properties of conductive polymer films, their porosity is affected by ion exchange, which significantly reduces the protective capacity of the resulting film [15]. In order to improve the corrosion characteristics of polymer coatings, it is necessary to block the pores on their surface in order to slow down ion exchange processes. Therefore, to solve these problems, copolymerization of the main monomer with other monomers, stepwise coating or doping with organic and inorganic components (composite coating) have been reported as some of the methods being used. The introduction of composites into the matrix of polymer, alloying is the most optimal way to obtaining polymer coatings with a clear structure, high conductivity and high anti-corrosion properties [16–18].

In this study, the electrochemical synthesis of POA polymer and POA–MoO<sub>4</sub><sup>2-</sup> composite on steel from aqueous oxalic acid was carried out using cyclic voltammetry. The effect of MoO<sub>4</sub><sup>2-</sup> anions on the electropolymerization process, corrosion properties and morphological characteristics of the resulting coatings are studied and reported.

## 2. Experimental procedure

### 2.1. Materials and methodology

o-Anisidine (AO, 99.8%) was supplied by Sigma Aldrich (Germany) and stored at 5 °C before use. Chemically pure oxalic acid dehydrate, sodium molybdate (Na<sub>2</sub>MoO<sub>4</sub>·2H<sub>2</sub>O) and chemically pure sodium chloride (NaCl) are used as received. Electropolymerization and corrosion studies were carried out on steel grade CT3.

The aqueous solution of oxalic acid (H<sub>2</sub>C<sub>2</sub>O<sub>4</sub>) was used as a supporting electrolyte. The concentrations of H<sub>2</sub>C<sub>2</sub>O<sub>4</sub> and o-anisidine were kept constant at 0.30 M and 0.10 M respectively.

The preparation of the steel surface (S = 0.1256 cm<sup>2</sup>) was carried out mechanically using a MoPaO 160 Dual speed Grinder Polisher and abrasive paper with sizes 1500, 2000, 2500, then cleaned in an ethanol solution, double-distilled water.

### 2.2. Electropolymerization of POA Coating + POA–MoO<sub>4</sub><sup>2-</sup> on CT3

Electrochemical polymerization of POA and POA MoO<sub>4</sub><sup>2-</sup> coatings on steel was carried out by cyclic voltammetry in a three-electrode electrochemical cell using a potentiostat-galvanostat

AUTOLAB PGSTAT (Netherlands). The working electrode was CT3 steel with an area of 0.1256 cm<sup>2</sup>. The counter electrode was a platinum plate and the reference electrode was Ag/AgCl electrode. Compositions of electrolytes for different coatings were prepared separately in 0.30 M oxalic acid solution containing, 0.10 M o-anisidine, 0.10 M o-anisidine + 0.01M Na<sub>2</sub>MoO<sub>4</sub>. A sweep rate of 20 mV/s and the number of cycles 20 were chosen as optimal electropolymerization conditions).

### 2.3. Corrosion tests

The polarization measurements were carried out in the potential range -0.30 V to 0.30 V of the stationary value with a sweep rate 2 mV/s. The potentiodynamic polarization curves were evaluated using NOVA software. The corrosion potential (E<sub>corr</sub>), corrosion current density (j<sub>corr</sub>), and corrosion rate [CR (mm/year)] were calculated based on Batler-Former equation. All the measurements were repeated at least three times, and good reproducibility of the results was observed.

### 2.4. Surface analyses

Quanta 200i 3D scanning electron microscope (SEM, FEI, United States) with different magnification from \*2000 to \*50000 and ZEISS Axio Vert. A1 Inverted Microscope (Carl Zeiss Microscopy, Germany) were used to investigate morphological characteristics and composition of POA and POA–MoO<sub>4</sub><sup>2-</sup> coatings.

## 3. Results and discussion

### 3.1. Electrochemical synthesis

As shown in Fig. 1a, b, the cyclic voltammograms of the electropolymerization of the first, second and third cycles, as well as the cyclic voltammograms of electropolymerization at 1, 2, 3, 5, 10, 20 times scanning on steel from an aqueous solution of 0.10 M POA + 0.30 M H<sub>2</sub>C<sub>2</sub>O<sub>4</sub>. In the first scan, peak A is observed at a potential (- 0.30 V) (vs. Ag/AgCl), which could be explained as a result of the dissolution of iron (Eq. 1),



Anodic current peaks at potentials 0.65 V (peak B) and 1.15 V (peak C) (vs. Ag/AgCl) are characteristic peaks of anisidine oxidation. The anodic

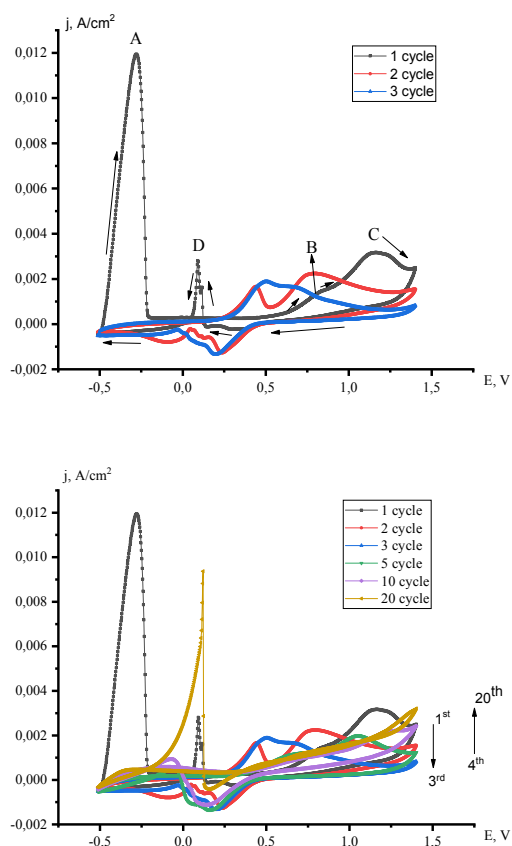


Fig. 1. Cyclic voltammograms: a – 1, 2, 3; b – 1, 2, 3, 5, 10, and 20 cycles that were obtained during the electrochemical synthesis of POA film on steel from 0.30 M  $\text{H}_2\text{C}_2\text{O}_4$ .

peak observed at approximately 0.65 V characterizes the POA transition between leucoemeraldine and the partially oxidized emeraldine state, and the anodic peaks at about 1.15 V correspond to the transition of the conductive form of emeraldine to the pernigraniline state [19, 20]. In subsequent cycles, the first anodic peak is not observed, since the mild steel is partially covered with a layer of polymer, which helps in inhibiting the mild steel dissolution.

Starting from the second cycle, there is a significant decrease in the current density for each polymerization process, which proves the polymerization of the monomer due to the growth of the polymer chain. In addition, a new anodic peak may be observed at a potential of 0.37 V (vs. Ag/AgCl), characterizing the POA oxidation. With an increase in the number of cycles, it is possible to obtain cycles as during the second scan. Already after the fourth scan, the cyclic voltammogram did not show any clear or defined oxidation peaks (Fig. 1b). During the reverse cycle, the anodic current

density sharply decreases and at a potential of 0.1 V (peak D) (vs. Ag/AgCl), a possible peak in the reduction of the oxalate ion is observed (Eq. 2):



The polymerization of POA in the presence of  $\text{MoO}_4^{2-}$ , oxidation peaks at potentials of 0.65 and 1.15 V (vs. Ag/AgCl) are observed, which are characteristic of o-anisidine oxidation peaks (Fig. 2a, b). It was found that the current density in the case of electropolymerization of POA –  $\text{MoO}_4^{2-}$  is higher than for POA at the initial scanning cycles, which indicates more favorable oxidation conditions and the growth rate of the POA –  $\text{MoO}_4^{2-}$  coating as compared to POA. Comparison of the cyclic voltammograms of POA (Fig. 1a, b) with POA –  $\text{MoO}_4^{2-}$  (Fig. 2a, b) shows that the current density at a potential of 0.1 V (vs. Ag/AgCl) is lower than the POA polymerization current densities, this can be explained by parallel reduction oxalate and molybdate ions.

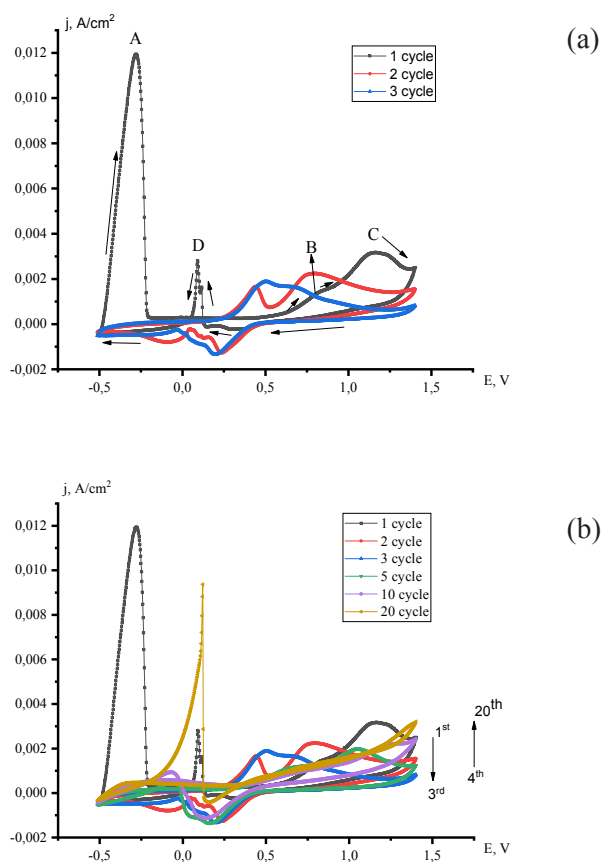


Fig. 2. Cyclic voltammograms: a – 1, 2, 3; b – 1, 2, 3, 5, 10, 20 cycles that were obtained during the electrochemical synthesis of POA –  $\text{MoO}_4^{2-}$  film on steel from 0.30 M  $\text{H}_2\text{C}_2\text{O}_4$ .

### 3.2. Corrosion protection tests

Protective characteristics of the corrosion of CT3 steel were determined by taking polarization curves in a sea water solution. Figure 3 indicates the polarization curves of oxidation of steel without and with POA and POA – MoO<sub>4</sub><sup>2-</sup> coatings in a solution of 3.5% NaCl at 25 °C. The calculation of the kinetic parameters was based on the Butler-Volmer equation, the values of which are presented in Table 1. The protective effect of the obtained films was calculated using the next equation:

$$Z = \frac{j_{corr}^0 - j_{corr}^i}{j_{corr}^0} * 100\%$$

$j_{corr}^0$  and  $j_{corr}^i$  – corrosion current density of samples in 3.5% NaCl solution, without and with electropolymerized coatings, A/cm<sup>2</sup>, respectively.

Table 1 indicates that the presence of a film on the steel top leads to a significant decrease in  $j_{corr}$  and increase in protection effects Z%. The corrosion rate of MS without coating is 7 and 29 times higher than in POA and POA – MoO<sub>4</sub><sup>2-</sup>, giving protection effects of 75.15 and 97.39%, respectively. The positive shift in the  $E_{corr}$  values supports the better protection of CT3 when its top is covered with a POA – MoO<sub>4</sub><sup>2-</sup> film. Due to the higher protective effect, the  $j_{corr}$  values for POA – MoO<sub>4</sub><sup>2-</sup> coatings are lower than those for bare uncoated mild steel. Thus, for MoO<sub>4</sub><sup>2-</sup>, a straight passivator, which is capable to reinforce, extend and restore the passive coat for better corrosion protection. Protection characteristics for different coatings correspond to the order MS/POA – MoO<sub>4</sub><sup>2-</sup> > MS/POA > bare MS.

To confirm the corrosion stability of polymer composite films, potentiodynamic polarization curves (Fig. 4) of composite coatings were obtained at different exposure times in a 3.5% NaCl solution. Samples of the obtained POA – MoO<sub>4</sub><sup>2-</sup> films were tested after 1, 2, 4, 8 h of exposure time in 3.5% chloride-containing media. By increasing the immersion time, it is observed that there is a

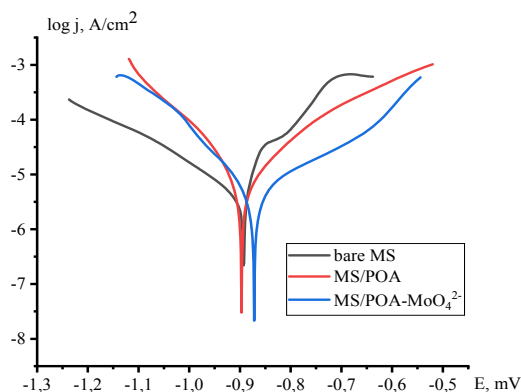


Fig. 3. Polarization curves of bare MS, MS/POA and POA – MoO<sub>4</sub><sup>2-</sup> in 3.5% NaCl solution.

in decrease in corrosion resistance and decrease in protection effect (Table 2).

As can be seen from Table 2, after 1 h of immersion of the composite coating, the corrosion rate is 0.017 mm/year. This value is lower than the corrosion rate of steel with POA – MoO<sub>4</sub><sup>2-</sup> 0.037 mm/year (Table 1) without immersion. This phenomenon is explained by the presence of corrosive products on the electrode surface by their synergistic effect, which improves the anticorrosive characteristics. Despite this, with an increase in immersion time from 2 to 8 h, the corrosion rate increases to 0.025 and 0.330 mm/year, respectively. As the corrosion rate increases, the protective effect of the coating decreases accordingly.

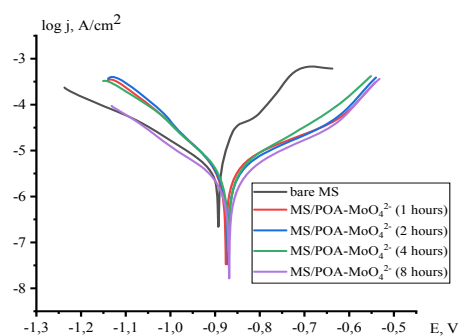


Fig. 4. Polarization curves of POA – MoO<sub>4</sub><sup>2-</sup> coating in different exposure time, 1, 2, 4, 8 h in 3.5% NaCl solution.

**Table 1**  
Protective characteristics of bare MS, MS+POA, MS+POA+ MoO<sub>4</sub><sup>2-</sup> in 3.5% NaCl at 25 °C

	$E_{corr}$ , mV	$j$ , $\mu\text{A}/\text{cm}^2$	R, kOhm	$v$ , mm/year	Z, %
Bare MS	-893.360	98.92	2.37	1.150	-
MS+POA	-897.220	24.58	3.17	0.290	75.15
MS+POA+ MoO <sub>4</sub> <sup>2-</sup>	-872.090	2.58	7.23	0.037	97.39

**Table 2**  
Protective characteristics of POA – MoO<sub>4</sub><sup>2-</sup> in 1, 2, 4, 8 h of exposure. Time in 3.5% NaCl at 25 °C

	E <sub>corr</sub> , mV	j, μA/cm <sup>2</sup>	R, kOhm	v, mm/year	Z, %
Bare MS	-893.360	98.92	2.37	1.150	-
1 h	-874.960	1.5	10.43	0.017	98.8
2 h	-871.730	2.19	10.35	0.025	97.9
4 h	-870.050	21.52	8.22	0.250	78.2
8 h	-871.230	28.50	7.53	0.330	71.2

### 3.2. Surface characterization and EDAX analysis

Figure 5a shows an SEM micrograph of a bare electrode with a relatively uniform surface and a crystalline interface. In Fig. 5b the electrode top is found coated with relatively non-uniform and POA granular when compared with POA – MoO<sub>4</sub><sup>2-</sup> film

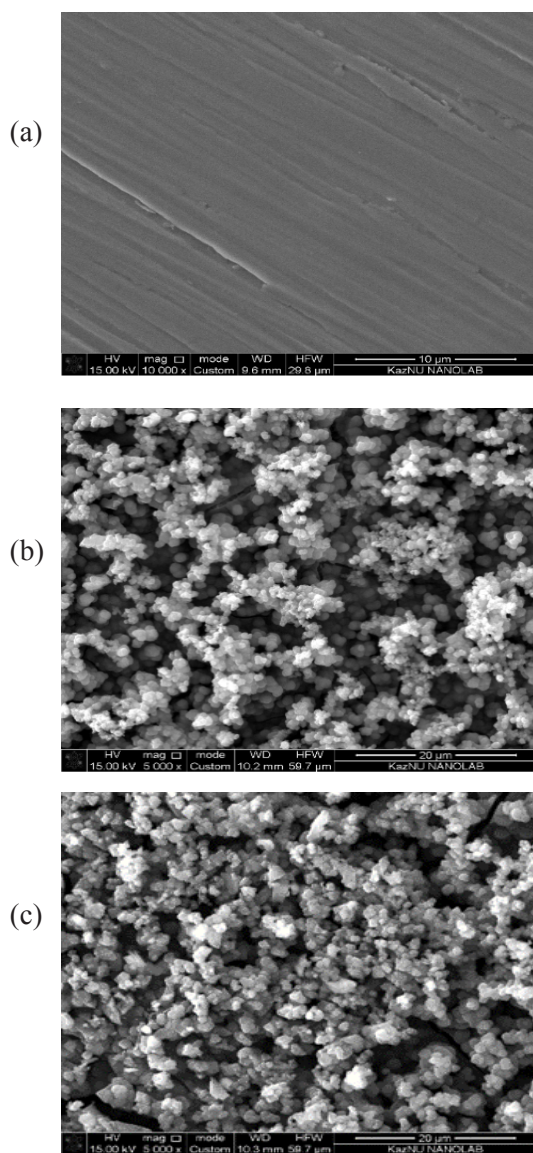


Fig. 5. SEM images: a – CT3; b – POA; c – POA – MoO<sub>4</sub><sup>2-</sup> coatings on CT3 steel, without exposure time, 20 μm.

(Fig. 5c). It is observed the crystals have different sizes ranging from 0.96 to 1.07 μm (Fig. 6a) and, are randomly arranged. A visible observation shows the presence of a dark green POA coating on the top of CT3.

Electrochemical passivation POA – MoO<sub>4</sub><sup>2-</sup> steel coatings allows to obtain hard coatings from dark green to black color on the surface of steel. After the incorporation of molybdate ions into the polymer matrix, POA – MoO<sub>4</sub><sup>2-</sup> coatings became denser with small aggregated particles. The denser the layer, the better the metal is protected from the influence of aggressive media. During polymerization with molybdate, the structure of the coating is preserved as in the case of POA, in addition, the length of individual crystals increases to 1.15 μm (Fig. 6b). POA – MoO<sub>4</sub><sup>2-</sup> film has a relatively sleek surface morphology, and indicated by the presence of grains of different size.

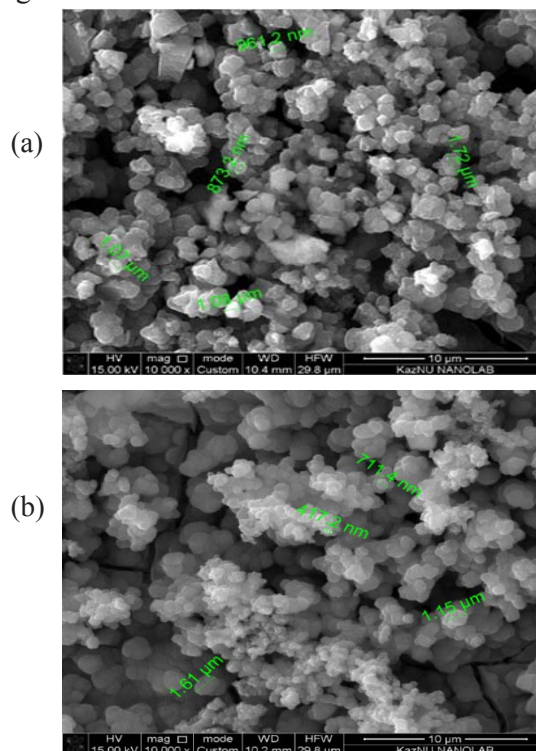


Fig. 6. SEM images: a – CT3; b – POA; c – POA – MoO<sub>4</sub><sup>2-</sup> films on CT3, without exposure time, 10 μm.

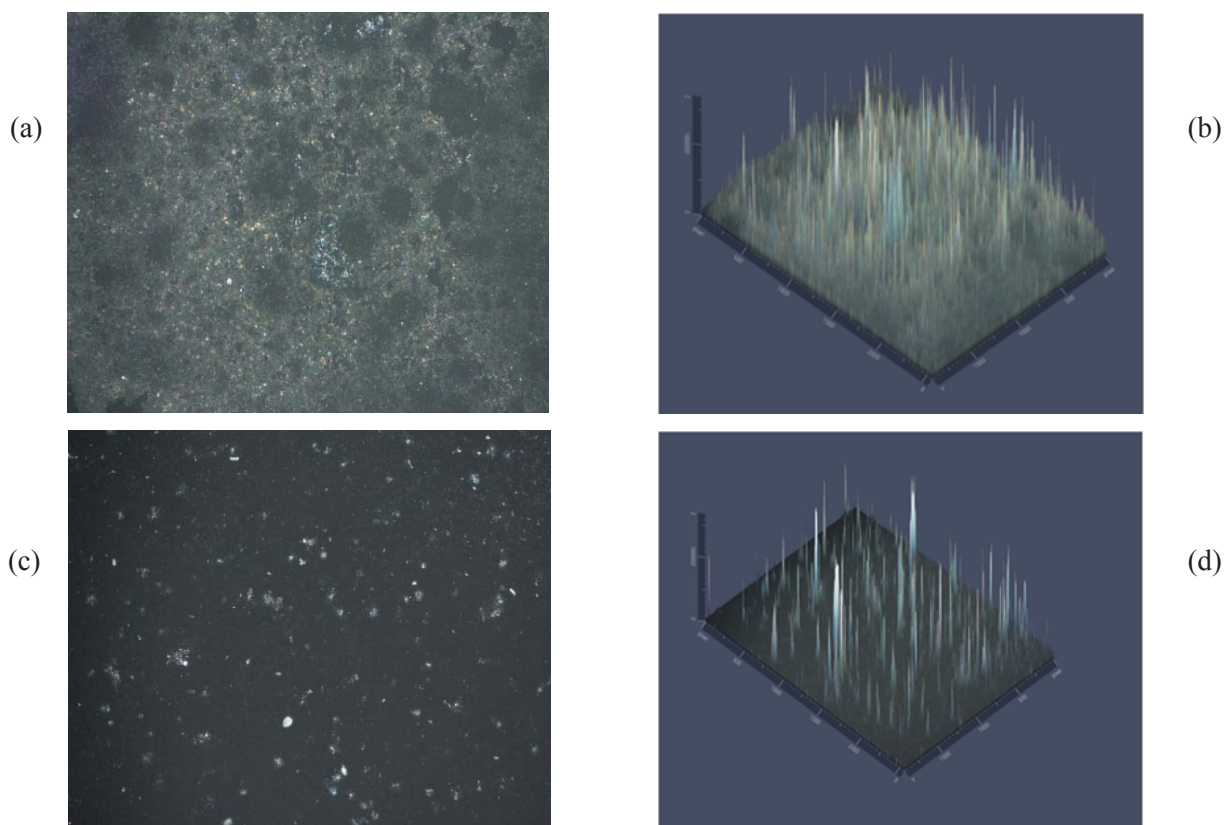


Fig. 7. Digital and stereo images of POA (a, c, respectively) and POA – MoO<sub>4</sub><sup>2-</sup> (b, d, respectively) coatings on CT3, \*100 magnification.

Digital images of the POA and POA – MoO<sub>4</sub><sup>2-</sup> composite films obtained on the MS electrode are shown in Fig. 7. In the comparison of the obtained images (7a, c), the POA images differ from those for composite films. POA films are gray, which could be explained by the presence of depressions (pits) in the image that proved that the coating is loose. In addition, the gray color describes the presence of a passivating FeC<sub>2</sub>O<sub>4</sub> film under the polymer. When considering composite films, it can be seen that the color of the films becomes dark gray, which is associated with the effect of molybdate on the morphol-

ogy of composite films. The stereo images shown in Fig. 7b, d indicate a more uniform and homogeneous nature of the POA – MoO<sub>4</sub><sup>2-</sup> coatings than for POA. This confirms the correlation of these results compared to the previously obtained SEM analysis results.

To confirm the reliability of the SEM results and to determine the composition of the resulting films was performed by EDAX analysis (Fig. 8). As can be seen from the results, the POA coating consists of C, O, Fe, and the POA – MoO<sub>4</sub><sup>2-</sup> film contains C, O, Fe, Mo, Na elements.

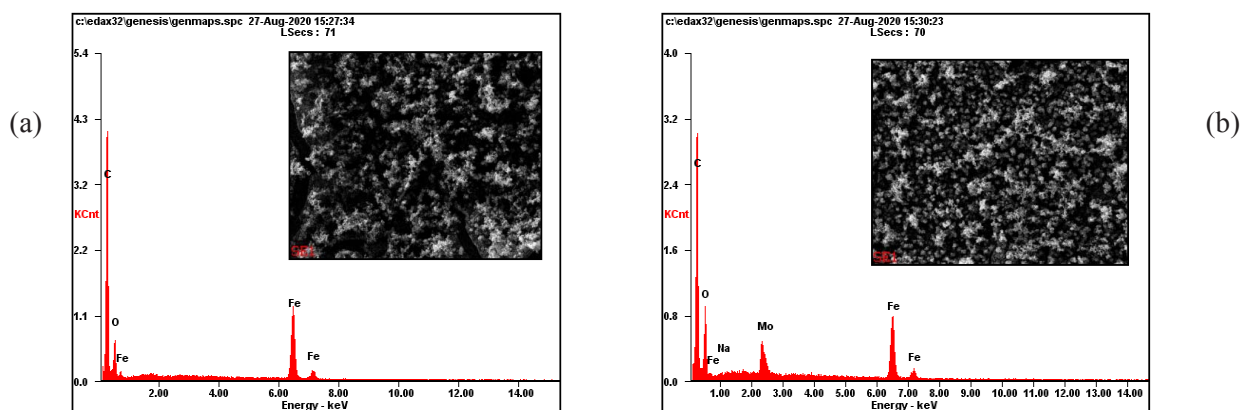


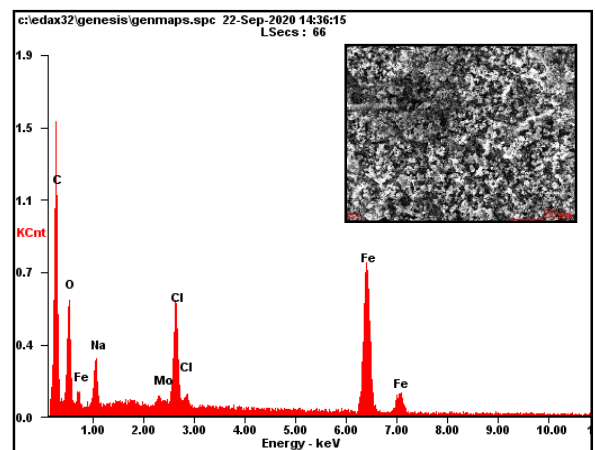
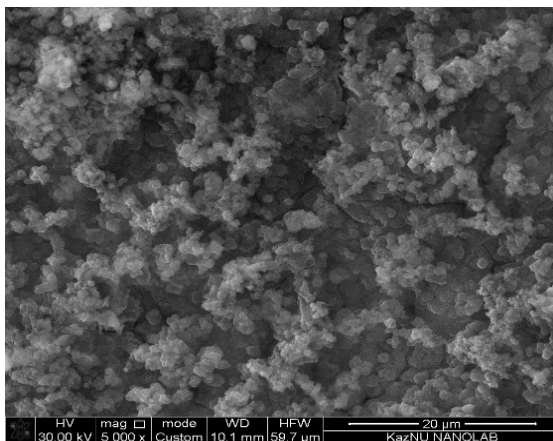
Fig. 8. EDAX spectra: a – POA; b – POA – MoO<sub>4</sub><sup>2-</sup>.

**Table 3**  
Comparison of composition of POA and  
POA – MoO<sub>4</sub><sup>2-</sup> coatings on mild steel

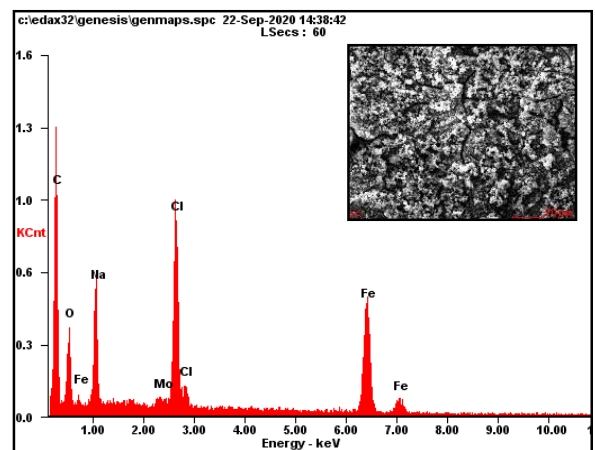
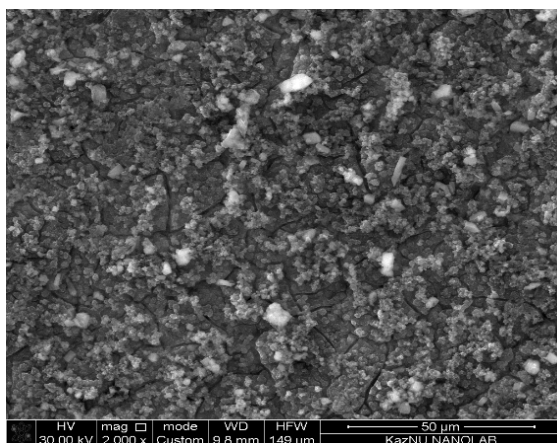
	W, %	
	POA	POA – MoO <sub>4</sub> <sup>2-</sup>
C	67.74	63.56
O	11.36	15.88
Fe	20.89	15.60
Mo	-	4.77
Na	-	0.19
Total	100.00	100.00

The results of the EDAX analysis are shown in Table 3. The presence of Mo in the composite coatings was shown, which, apparently, leads to the formation of complex compounds of Mo and Fe during the electrochemical synthesis. In addition, the presence of Mo improves the protective effects of the obtained polymer film on CT3 due to the formation of bulk products in the pores of the POA coating.

Figure 9 shows SEM micrographs and EDAX spectra of POA – MoO<sub>4</sub><sup>2-</sup> coatings after 1, 2, 4, 8 h of exposure in 3.5% NaCl solution. It can be seen that after immersion of the sample, some corrosion products are formed on the surface of the composite coating, which increase with immersion time. The part of the POA – MoO<sub>4</sub><sup>2-</sup> coating was noticeably localized and damaged, and the corrosion products spread over the entire surface due to cracks, which causes ion exchange between the electrolyte and the coating, thereby reducing the protective effect. Over time, defects and pores appear, which facilitate the penetration of the electrolyte into the depth of the film, and, accordingly, the charge transfer reaction happens between coating and metal interface. This process leads to the occurrence of corrosion with its subsequent spread under the polymer coating. The reduction properties of conducting polymer allow passivate small porosity, which forms under coating during the exposure time, but the including of MoO<sub>4</sub><sup>2-</sup> ions in a polymer matrix helps to achieve a uniform coating.



(a)



(b)

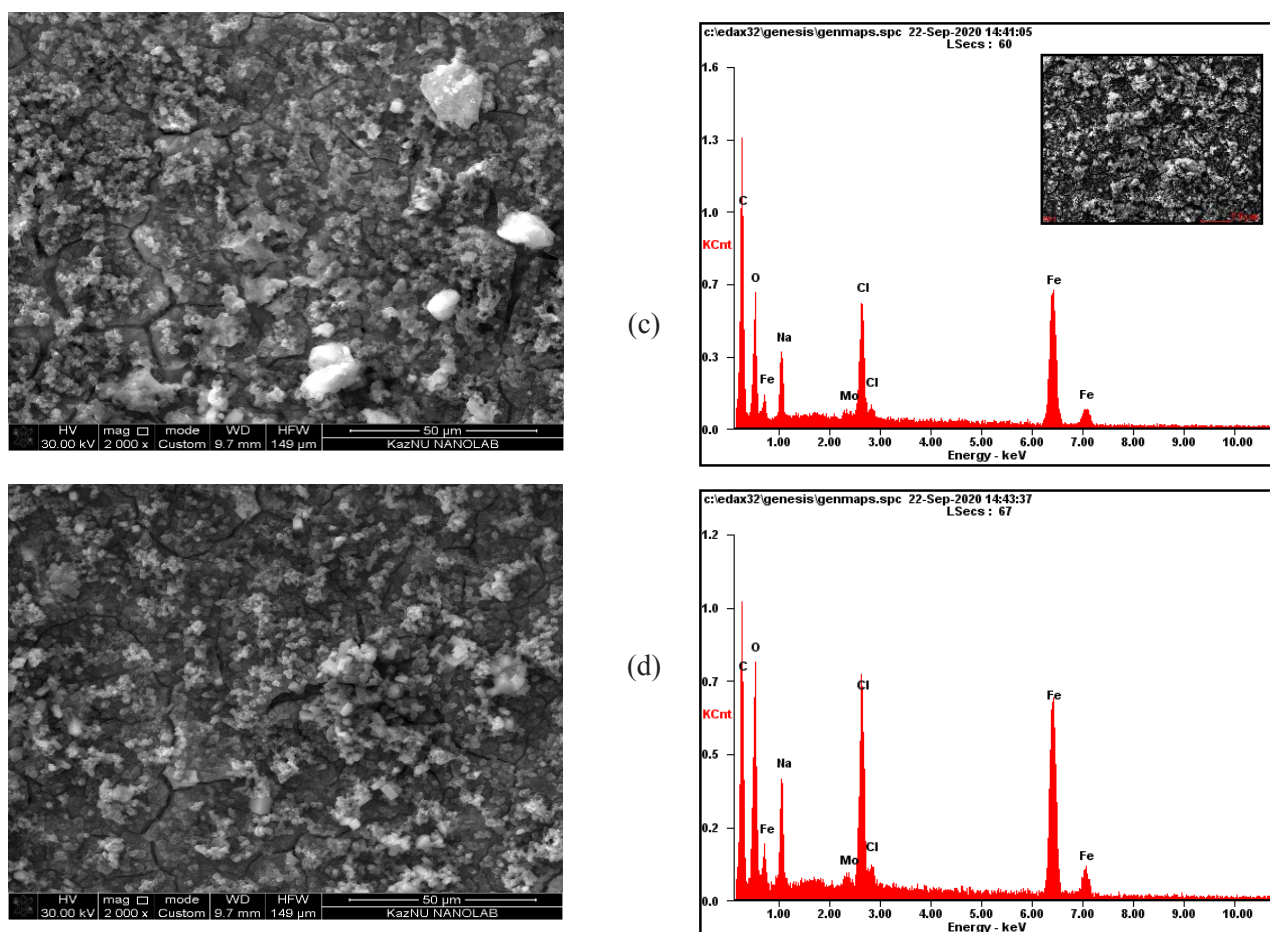


Fig. 9. SEM images and EDAX spectra of POA – MoO<sub>4</sub><sup>2-</sup> coating in 3.5% NaCl in different exposure time: a – 1 h; b – 2 h; c – 4 h; d – 8 h, 2 μm.

## Conclusion

In this study, POA and POA – MoO<sub>4</sub><sup>2-</sup> films were synthesized on CT3 steel by the cyclic voltammetry method. The EDAX results indicate the availability of Mo in the structure of the composite coating and the SEM images indicate the homogeneous and compact structure of the composite. The kinetic parameters of POA and POA – MoO<sub>4</sub><sup>2-</sup> films in 3.5% NaCl solution were calculated from the polarization curves. The corrosion rate of POA – MoO<sub>4</sub><sup>2-</sup> composite film was found to be 29 times slower than uncoated mild steel, and the protective effect was 97.39%. Increased exposure time POA – MoO<sub>4</sub><sup>2-</sup> composite coatings in 3.5% NaCl solution led to decreased resistance with raised in current density, which is consistent with electrochemical measurements.

## Acknowledgments

This research has been funded by the Science Committee of the Ministry of Education and Science of the Republic of Kazakhstan (Grant No. AP05134571).

## References

- [1]. C.-H. Chang, T.-C. Huang, C.-W. Peng, T.-C. Yeh, H.-I. Lu, W.-I. Hung, C.-J. Weng, T.-I. Yang, J.-M. Yeh, *Carbon* 50 (2012) 5044–5051. DOI: [10.1016/j.carbon.2012.06.043](https://doi.org/10.1016/j.carbon.2012.06.043)
- [2]. D. Kowalski, M. Ueda, T. Ohtsuka, *Corros. Sci.* 49 (2007) 1635–1644. DOI: [10.1016/j.corsci.2006.08.018](https://doi.org/10.1016/j.corsci.2006.08.018)
- [3]. H. Shokry, *Chem. Met. Alloys* 2 (2009) 202–210. DOI: [10.30970/cma2.0108](https://doi.org/10.30970/cma2.0108)
- [4]. R. Babaei-sati, J. Basiri, M. Vakili-azghandi, *Synthetic Met.* 247 (2018) 183–190. DOI: [10.1016/j.synthmet.2018.12.009](https://doi.org/10.1016/j.synthmet.2018.12.009)
- [5]. I.B. Obot, A. Madhankumar, S.A. Umoren, Z.M. Gasem, *J. Adhes. Sci. Technol.* 29 (2015) 2130–2152. DOI: [10.1080/01694243.2015.1058544](https://doi.org/10.1080/01694243.2015.1058544)
- [6]. S.A. Umoren, M.M. Solomon, *J. Environ. Chem. Eng.* 5 (2017) 246–273. DOI: [10.1016/j.jece.2016.12.001](https://doi.org/10.1016/j.jece.2016.12.001)
- [7]. P.P. Deshpande, N.G. Jadhav, V.J. Gelling, D. Sazou, *J. Coat. Technol. Res.* 11 (2014) 473–494. DOI: [10.1007/s11998-014-9586-7](https://doi.org/10.1007/s11998-014-9586-7)
- [8]. M.I. Khan, A.U. Chaudhry, S. Hashim, M.K. Zahoor, M.Z. Iqbal, *Chem. Eng. Res. Bull.* 14 (2010) 73–86. DOI: [10.3329/ceerb.v14i2.5918](https://doi.org/10.3329/ceerb.v14i2.5918)

- [9]. J.W. Wu, T.L. Wang, W.C. Lin, H.Y. Lin, M.H. Lee, C.H. Yang, *Coatings* 8 (2018) 155. DOI: [10.3390/coatings8050155](https://doi.org/10.3390/coatings8050155)
- [10]. A.A. Ganash, F.M. Mahgoub, *Prot. Met. Phys. Chem.* 52 (2016) 555–561. DOI: [10.1134/S2070205116030114](https://doi.org/10.1134/S2070205116030114)
- [11]. Y. Ma, B. Fan, H. Liu, G. Fan, H. Hao, B. Yang, *Appl. Surf. Sci.* 514 (2019) 146086. DOI: [10.1016/j.apsusc.2020.146086](https://doi.org/10.1016/j.apsusc.2020.146086)
- [12]. M. Shabani-Nooshabadi, S.M. Ghoreishi, Y. Jafari, N. Kashanizadeh, *J. Polym. Res.* 21 (2014) 416–426. DOI: [10.1007/s10965-014-0416-5](https://doi.org/10.1007/s10965-014-0416-5)
- [13]. G. Bereket, E. Hür, Y. Şahin, *Prog. Org. Coat.* 54 (2005) 63–72. DOI: [10.1016/j.porgcoat.2005.06.002](https://doi.org/10.1016/j.porgcoat.2005.06.002)
- [14]. S. Chaudhari, A.B. Gaikwad, P.P. Patil, *Curr. Appl. Phys.* 9 (2009) 206–218. DOI: [10.1016/j.cap.2008.01.012](https://doi.org/10.1016/j.cap.2008.01.012)
- [15]. M. Ates, *J. Adhes. Sci. Technol.* 30 (2016) 1510–1536. DOI: [10.1080/01694243.2016.1150662](https://doi.org/10.1080/01694243.2016.1150662)
- [16]. R. Rajkumar, C. Vedhi, *Anti-Corros. Method. M.* 67 (2020) 305–312. DOI: [10.1108/ACMM-11-2019-2204](https://doi.org/10.1108/ACMM-11-2019-2204)
- [17]. S. Pourhashem, F. Saba, J. Duan, A. Rashidi, F. Guan, E.G. Nezhad, B. Hou, *J. Ind. Eng. Chem.* 88 (2020) 29–57. DOI: [10.1016/j.jiec.2020.04.029](https://doi.org/10.1016/j.jiec.2020.04.029)
- [18]. N. Jadhav, S. Kasisomayajula, V.J. Gelling, *Front. Mater.* 7 (2020) 1–7. DOI: [10.3389/fmats.2020.00095](https://doi.org/10.3389/fmats.2020.00095)
- [19]. A. Ray, G.E. Asturias, D.L. Kershner, A.F. Richter, A.G. MacDiarmid, A.J. Epstein, *Synthetic Met.* 29 (1989) 141–150. DOI: [10.1016/0379-6779\(89\)90289-0](https://doi.org/10.1016/0379-6779(89)90289-0)
- [20]. J. Stejskal, P. Kratochvíl, A.D. Jenkins, *Collect. Czech. Chem. Commun.* 60 (1995) 1747–1755. DOI: [10.1135/cccc19951747](https://doi.org/10.1135/cccc19951747)